

Mesoporous Heteropolyacid Nanorods for Heterogeneous Catalysis in Polysaccharide Conversion

Jiaying Song, Yiming Li, Xueyan Zhang, Dan Zhang, Zijiang Jiang,* and Xiaohong Wang*

Mesoporous heteropolyacid (HPA) nanorods having a composition of $[C_{16}H_{33}N(CH_3)_3]_xH_{3-x}PW_{12}O_{40}$ ((CTA) $_x$ H $_{3-x}$ PW, $x = 1, 2,$ and 3) were synthesized by surfactant encapsulation and were evaluated for their catalytic activity in cellulose hydrolysis. The (CTA)H $_2$ PW nanorods were found to be most active with 57.2% yield of 5-hydroxymethylfurfural (5-HMF) at ~100% conversion in water/methyl isobutyl ketone (MIBK) biphasic system, which was higher than (CTA)H $_2$ PW nanosphere at 140 °C for 11 h. The yields of 5-HMF and glucose were obtained as 4.5% and 54.3% at 160 °C for 8 h in water system, respectively. (CTA)H $_2$ PW nanorods showed higher tolerance to such feedstocks as lignocellulose, *i.e.* corn straw with 19.8% and 8.3% yields for glucose and xylose at 35.4% conversion in water. Moreover, (CTA)H $_2$ PW nanorods showed higher stability and long duration with ten times reuse. (CTA)H $_2$ PW nanorods presented higher efficiency and reusability in conversion of cellulosic biomass.

Keywords: Heteropolyacid; Mesoporous; Nanorod; Hydrolysis; Cellulose; 5-HMF

Contact information: Key Lab of Polyoxometalate Science of Ministry of Education, Faculty of Chemistry, Northeast Normal University, Changchun 130024, P. R. China;

* Corresponding author: wangxh665@nenu.edu.cn

INTRODUCTION

5-Hydroxymethylfurfural (5-HMF) is an important bioplateform chemical that has been produced from the conversion of monosaccharides or polysaccharides (Delidovich *et al.* 2014). Directly transforming cellulose to 5-HMF might be more economical and energy efficient without competing with the edible sugars. The process contains three cascade reactions: hydrolysis to glucose, isomerization to fructose, and final dehydration to 5-HMF in the presence of acidic catalysts (Li *et al.* 2018). Compared with homogeneous acids (HCl or H $_2$ SO $_4$), heterogeneous catalysts might be more environmentally friendly with easy separation, recyclability, and no corrosion (Jing *et al.* 2018). The difficulty in mass-transfer between solid catalysts and solid cellulose might hinder their application in 5-HMF production.

Heteropolyacids (HPAs) are acidic catalysts with strong Brønsted acidity; they have been widely used in cellulose conversion (Geboers *et al.* 2010; Fan *et al.* 2011; Chambon *et al.* 2011; Palkovits *et al.* 2011; Sun *et al.* 2012; Qu *et al.* 2012; Deng *et al.* 2012; Tsubaki *et al.* 2013; Xie *et al.* 2014; Zhao *et al.* 2014; Zhao *et al.* 2015; Sun *et al.* 2015a; Kumar *et al.* 2016; Zhao *et al.* 2018a; Zhang *et al.* 2018; Almohalla *et al.* 2018; Zhang *et al.* 2019). To overcome the mass-transfer difficulty, surfactant-type HPAs were developed and have shown benefits including concentrating substrates and providing special surroundings by their hydrophobic tail and hydrophilic head (Li *et al.* 2004; Tang *et al.* 2012; Lü *et al.* 2010; Zhang *et al.* 2010; Cheng *et al.* 2011; Zhao *et al.* 2011; Zhang

et al. 2011; Zheng *et al.* 2013; Lu *et al.* 2015; Sun *et al.* 2015b; Sun *et al.* 2016; Zhang *et al.* 2016a). The compounds $[\text{C}_{16}\text{H}_{33}\text{N}(\text{CH}_3)_3]\text{H}_2\text{PW}_{12}\text{O}_{40}$ ((CTA) H_2PW), $\text{Cr}[(\text{DS})\text{H}_2\text{PW}_{12}\text{O}_{40}]_3$ (DS is the abbreviation of dodecyl sulfate), $(\text{CTA})\text{H}_3\text{PW}_{11}\text{CrO}_{39}$, $(\text{CTA})\text{H}_4\text{PW}_{11}\text{TiO}_{40}$, $[\text{HOCH}_2\text{CH}_2\text{N}(\text{CH}_3)_3]\text{H}_2\text{PW}_{12}\text{O}_{40}$ and $[\text{HOCH}_2\text{CH}_2\text{N}(\text{CH}_3)_3]\text{H}_4\text{AlW}_{12}\text{O}_{40}$ all showed good activity in cellulose transformation to glucose, 5-HMF, or levulinic acid (LA), which the best yields of 5-HMF, LA and glucose were obtained as 75.0%, 74.8%, and 75.9% upon $[\text{HOCH}_2\text{CH}_2\text{N}(\text{CH}_3)_3]\text{H}_2\text{PW}_{12}\text{O}_{40}$ and $[\text{HOCH}_2\text{CH}_2\text{N}(\text{CH}_3)_3]\text{H}_4\text{AlW}_{12}\text{O}_{40}$, respectively (Zhang *et al.* 2016a; Sun *et al.* 2016). However, these surfactant-type HPAs did not exhibit porous characteristics, which could provide more reacting room for transformations. Various solid hybrids with porous structure have been found to be active for cellulose to 5-HMF (Zhang *et al.* 2016b; Zhang *et al.* 2017; Zhao *et al.* 2018b). In this concept, surfactant-type HPAs with porous structure would be designable.

Surfactant-type HPAs had been developed to fabricate different architectures with tunable morphologies including one-dimensional wires (Kang *et al.* 2004) and fibers (Carraro *et al.* 2008), two-dimensional thin-films (Liu *et al.* 2002; Bao *et al.* 2009) and disks (Nisar *et al.* 2009a), and three-dimensional vesicles (Zhang *et al.* 2008; Bu *et al.* 2009), spheres (Li *et al.* 2007; Nisar *et al.* 2009b), tubes (Ritchie *et al.* 2009), flowers (Nisar *et al.* 2009c), and cone (Nisar *et al.* 2011). A surfactant-type HPA with nanorod morphology and porous properties was designable due to the well-matched linear shape and porous cavity for interactions between active sites and cellulose (Zhang *et al.* 2016c).

Based on the above, surfactant-type HPAs $(\text{CTA})_x\text{H}_{3-x}\text{PW}$ nanorod with mesoporous structure had been synthesized through simply controlling their initial usages. Such nanorod showed enhanced activity in cellulose hydrolysis either in water or in $\text{H}_2\text{O}/\text{MIBK}$ biphasic system. Higher efficiency can be attributed to their one-dimensional morphology, which is a good match to linear cellulose, porous structure favoring for the reaction. Moreover, $(\text{CTA})_x\text{H}_{3-x}\text{PW}$ nanorod showed easily separation compared to their spherical species. The cellulose or even lignocellulose was hydrolyzed into 5-HMF or glucose in $\text{H}_2\text{O}/\text{MIBK}$ biphasic system or in water systems upon $(\text{CTA})\text{H}_2\text{PW}$ due to its stronger Brønsted acidity and special nanorod morphology, which also showed higher stability and longer duration.

EXPERIMENTAL

Materials

Microcrystalline cellulose (white, average particle size 50 μm) was obtained from Beijing InnoChem Science & Technology Co., Ltd. All other reagents were of AR grade and used without further purification. The 3,5-dinitrosalicylic acid (DNS) reagent was prepared according to ref (Cowan *et al.* 2001). $\text{H}_3\text{PW}_{12}\text{O}_{40}$ was prepared based on Duan *et al.* (2013).

Characterization

The elemental analysis was obtained using a Leeman Plasma Spec (I) ICP-ES and a P-E 2400 CHN elemental analyzer. FTIR spectra were recorded on a Nicolet Magna 560 IR spectrometer (KBr discs) in the 4000 to 400 cm^{-1} region. X-ray diffraction (XRD) patterns of the catalysts were carried out using a Japan Rigaku Dmax 2000 X-ray diffractometer with $\text{Cu K}\alpha$ radiation ($\lambda = 0.154178 \text{ nm}$) (Rigaku Corporation, Japan).

UV-vis spectra (200-600 nm) were recorded on a Cary 500 UV-vis-NIR spectrophotometer. DR-UV-vis spectra (200-600 nm) were obtained on a UV-2600 UV-vis spectrophotometer (Shimadzu). The ^{31}P NMR spectra of the catalysts were achieved with a Bruker AM 400 spectrometer at 161.9 MHz. SEM images were determined by a SU8010 scanning electron microscope. The energy dispersive X-ray analysis (EDX) was performed to calculate the contents of P, W, O, N, and C elements. TEM micrographs were recorded on a Hitachi H-600 transmission electron microscope. Brunauer-Emmett-Teller (BET) specific surface area, total pore volume and average pore width of the catalysts were determined by a N_2 physisorption experiment using an automatic gas adsorption system (ASAP 2020, Micromeritics Instrument Corp, USA) at $-196\text{ }^\circ\text{C}$. The sample was degassed at $90\text{ }^\circ\text{C}$ for 8 h before the physical adsorption of N_2 . The electro-potential variation was measured with an instrument of ZDJ-4B automatic potentiometric titration, using a BestLab Non-aqueous pH Titration electrode (Shanghai, China).

Chemical Tests

The acidic strength was measured by the titration according to the previous literature (Pizzio and Blanco 2007). The concentrations of 5-HMF and LA were determined on Agilent Technologies 7820A GC system fitted with an Agilent J&W Advanced capillary GC column (Shanghai, China). The concentration of glucose was measured in the aqueous phase by HPLC equipped with a refractive index detector (Shimadzu LC-10A, HPX-87H column) column at $35\text{ }^\circ\text{C}$. The mobile phase was H_2O with a flow rate of 0.5 mL/min at $75\text{ }^\circ\text{C}$. The concentration of xylose was measured by HPLC equipped with a refractive index detector using a UltimateXB-NH $_2$ ($4.6\text{ mm}\times 150\text{ mm}$, $5\text{ }\mu\text{m}$) column at $35\text{ }^\circ\text{C}$. The mobile phase was H_2O /acetonitrile ($1/4\text{ v/v}$) with a flow rate of 1.0 mL/min . The error bars were obtained as the standard deviation of three measurements, which were calculated based on the following:

$$S = \sqrt{\frac{1}{N-1} \sum_{i=1}^N (X_i - \bar{X})^2}.$$

Methods

50 mL of hexadecyltrimethylammonium bromide (CTAB) aqueous solution (20 mM) was added into 50 mL of $\text{H}_3\text{PW}_{12}\text{O}_{40}$ (HPW, 20 mM) with stirring. The white precipitate formed immediately. Then the mixture was kept still for 24 h . The white precipitate was separated and dried under vacuum at $50\text{ }^\circ\text{C}$. Then it was calcined at $200\text{ }^\circ\text{C}$ for 3 h , 72.3% yield. The other hybrids $(\text{CTA})_x\text{H}_{3-x}\text{PW}$ with different x values were synthesized using the same procedure except using $M_{\text{CTAB}}: M_{\text{HPW}} = 2: 1$ and $3: 1$, instead.

Catalytic Procedure

For the hydrolysis of cellulose into the 5-HMF in the double solvent MIBK/ H_2O system, the mixture cellulose (0.1 g), and the catalyst (0.09 mmol) were added to H_2O (0.5 mL) and MIBK (5 mL). Then they were placed in a steel autoclave for 11 h at $140\text{ }^\circ\text{C}$ under magnetic stirring (300 rpm). The reaction was stopped by rapidly cooling the reactor in an ice bath at $0\text{ }^\circ\text{C}$ for 30 min . After the temperature reached room temperature, the reaction solution formed three layers: the first layer was the organic phase which contained the desired product 5-HMF. The second layer was the aqueous phase that contained fructose and glucose. The third layer was solid which contained unreacted cellulose and the catalyst. The mixture was centrifuged, then washed three times with

water and ethanol, and dried under vacuum at 60 °C for 24 h. Repeated experiments only increased some fresh cellulose to 0.1 g as the initial amount due to the inability to separate the catalyst in the mixture from the unreacted cellulose and by-products humin by centrifugation. The total amount of the catalyst leaching after ten cycles of experiments was detected by UV-vis spectroscopy. Cellulose conversions (wt %) were determined by the difference between the cellulose weight before and after the reaction. The quantitative analyse of 5-HMF was determined by Gas Chromatograph (GC).

For the hydrolysis of cellulose in water, a mixture of cellulose (0.1 g) and catalyst (0.09 mmol) was added into water (7 mL). Then the mixture was heated at 160 °C in a steel autoclave lined with Teflon for 8 h with stirring (300 rpm). The reaction was stopped by rapidly cooling the reactor in an ice bath at 0 °C. After the temperature reached room temperature, the mixture was centrifuged to separate the catalyst and unreacted cellulose. Cellulose conversions (wt%) were determined by the change in cellulose weight before and after the reaction. 5-HMF was determined by HPLC (high-performance liquid chromatography). The concentration of glucose was measured in the aqueous phase by HPLC equipped with a refractive index detector (Shimadzu LC-10A, HPX-87H column) column at 35 °C. In both two systems, the conversion of sucrose, cellobiose, starch and corn straw was done in the same procedure as cellulose conversion.

Total Reducing Sugars (TRS) Analysis

A mixture that contained 2 mL of the DNS reagent and 1 mL of the reaction sample was heated for 2 min in a boiling water bath, then cooled to room temperature with flowing water, and mixed with deionized water to a volume of 25 mL. The color intensity of the mixture was measured in a UV757CRT model spectrophotometer at 540 nm. The concentration of total reducing sugars was calculated based on a standard curve obtained with glucose. (Cowan *et al.* 2001)

Adsorption Experiment

In order to confirm the adsorption capacity of the catalyst to cellulose, the adsorption experiment was conducted. During the adsorption experiment, a mixture of cellulose (0.1 g) and the catalyst (0.09 mmol) were mixed together in H₂O (5.5 mL) in a steel autoclave lined with Teflon at a 140 °C for 1 h. The powder solids were removed and dried in a vacuum of 60 °C. Then it was used to determine the adsorption of cellulose upon (CTA)_xH_{3-x}PW nanorod by IR spectroscopy.

RESULTS AND DISCUSSION

Characterization of the Catalysts

From the results of the elemental analysis (Table 1), the molar ratio of W and P in catalysts was P: W = 1: 12, corresponding to that with Keggin structure of PW₁₂O₄₀³⁻. The contents of C, H and N were inherent with the calculated values indicating the formula as (CTA)_xH_{3-x}PW₁₂O₄₀ (x = 1-3).

Figure 1 shows the IR spectra of the (CTA)_xH_{3-x}PW nanorods, giving the four characteristic peaks similar to their parent H₃PW₁₂O₄₀ (1075, 976, 899, and 796 cm⁻¹) (Deltcheff *et al.* 1983), indicating that the catalysts maintained the original heteropolyacid structure during reaction with CTAB. In addition, peaks of C-H stretching vibration at 2916 and 2845 cm⁻¹, and C-N at 1467 cm⁻¹ confirmed the presence of CTA⁺

in the hybrids. The characteristic peaks belonging to $\text{PW}_{12}\text{O}_{40}^{3-}$ anion shifted depending on the CTA^+ contents, showing the existence of anion-cation interaction between the polyoxometalate anion and CTA^+ . The Keggin structure of $(\text{CTA})_x\text{H}_{3-x}\text{PW}$ ($x = 1-3$) nanorod was further determined by DR-UV-vis spectroscopy, which presented one peak at 267 nm assigned to $\text{O} \rightarrow \text{W}$ charge transition (Fig. 2).

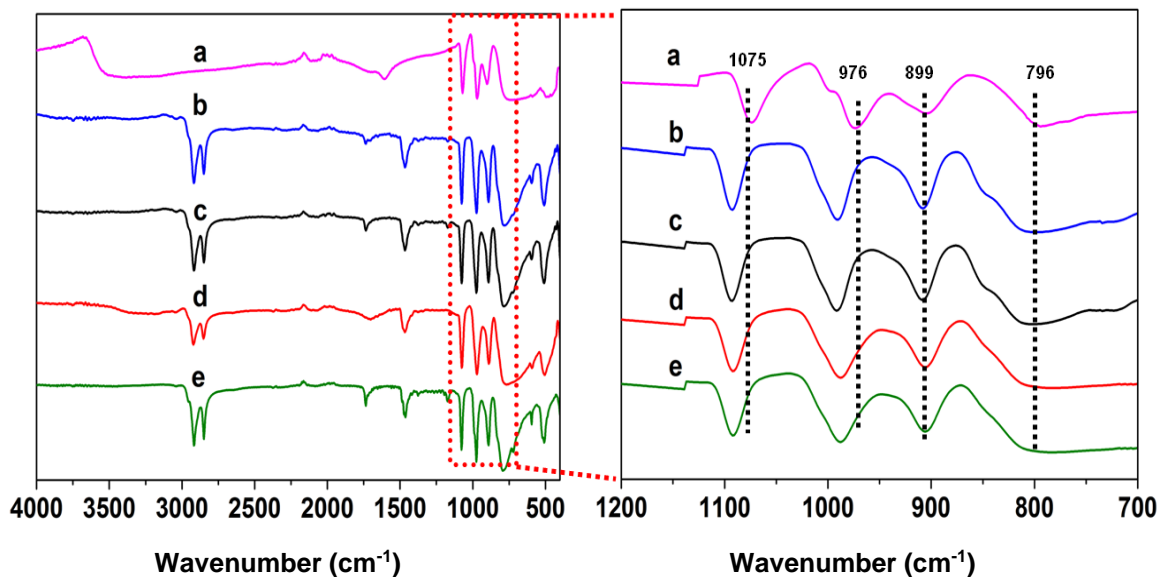


Fig. 1. IR spectra of (a) $\text{H}_3\text{PW}_{12}\text{O}_{40}$, (b) $(\text{CTA})\text{H}_2\text{PW}$ nanorod, (c) $(\text{CTA})_2\text{HPW}$ nanorod, (d) $(\text{CTA})_3\text{PW}$ nanorod, and (e) $(\text{CTA})\text{H}_2\text{PW}$ nanorod after the reaction

Table 1. Elemental Analysis, Total Acidity and Hydrolysis Activity ^a of H₃PW₁₂O₄₀ and (CTA)_xH_{3-x}PW Nanorod

Catalyst	Elementary results (calculated values in parenthesis)/wt %				Total acidity ^c (mmol/g)	MIBK/H ₂ O ^a			H ₂ O ^b		
	C	N	P	W		Con. (%)	5-HMF yields (%)	Glucose yields (%)	Con. (%)	5-HMF Yields (%)	Glucose yields (%)
H ₃ PW ₁₂ O ₄₀	-	-	1.10 (1.08)	76.58 (76.60)	1.78	91.2	47.2	14.2	80.6	18.2	47.8
(CTA) ₂ PW nanosphere	7.43 (7.21)	0.39 (0.44)	1.06 (0.98)	69.37 (69.73)	1.38	72.9	36.3	18.2	41.3	3.1	32.2
(CTA) ₂ PW nanorod	7.40 (7.21)	0.38 (0.44)	1.07 (0.98)	69.35 (69.73)	1.41	~100	57.2	17.6	64.8	4.5	54.3
(CTA) ₂ HPW nanorod	13.39 (13.24)	0.76 (0.81)	0.96 (0.90)	63.47 (63.99)	0.72	60.9	29.1	13.2	32.4	2.8	26.2
(CTA) ₃ PW nanorod	18.61 (18.35)	1.02 (1.13)	0.89 (0.83)	58.69 (59.13)	0.04	32.7	14.3	7.9	15.6	1.6	9.6
^a Reaction conditions: cellulose (0.1 g), MIBK (5 mL), H ₂ O (0.5 mL), 140 °C, 11 h, catalyst (0.09 mmol).											
^b Reaction conditions: cellulose (0.1 g), H ₂ O (7 mL), 160 °C, 8 h, catalyst (0.09 mmol).											
^c The total acidity was measured using potentiometric titration method.											

The XRD patterns of $\text{H}_3\text{PW}_{12}\text{O}_{40}$ and $(\text{CTA})_x\text{H}_{3-x}\text{PW}$ showed that all exhibited typical X-ray diffractograms of Keggin anion at 10.2° , 20.6° , 25.1° , 34.5° , and 53.7° , indicating the retain of the structure after reacting with CTAB (Fig. 3). And slight shifts for XRD of $(\text{CTA})_x\text{H}_{3-x}\text{PW}$ determined the existence of $(\text{CTA})_x\text{H}_{3-x}\text{PW}$ and no physical mixture of $\text{PW}_{12}\text{O}_{40}^{3-}$ anion and CTAB (Wang *et al.* 2016).

The ^{31}P MAS NMR spectrum of the $(\text{CTA})\text{H}_2\text{PW}$ nanorod gave one peak at -17.99 ppm (Fig. 4a) with some shift compared to its parent $\text{H}_3\text{PW}_{12}\text{O}_{40}$ (-15.6 ppm). This result confirmed the formation of $(\text{CTA})\text{H}_2\text{PW}$ nanorod and no physical mixture of CTA^+ and $\text{H}_3\text{PW}_{12}\text{O}_{40}$.

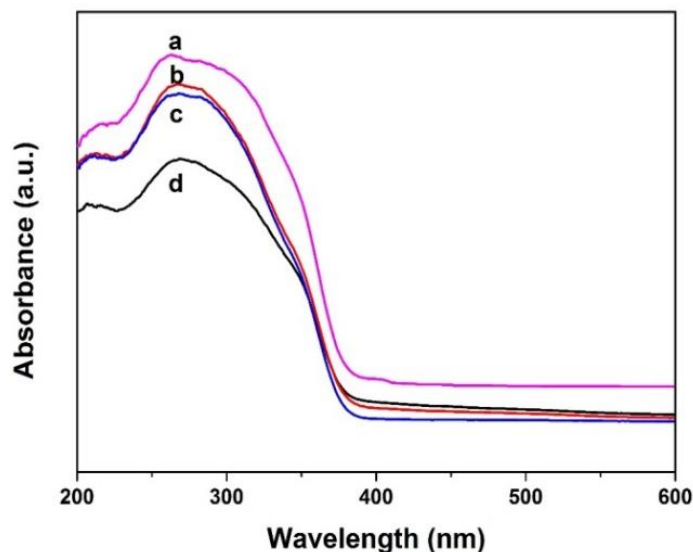


Fig. 2. DR-UV-vis spectra of the catalysts. (a) $\text{H}_3\text{PW}_{12}\text{O}_{40}$, (b) $(\text{CTA})\text{H}_2\text{PW}$ nanorod, (c) $(\text{CTA})_2\text{HPW}$ nanorod, and (d) $(\text{CTA})_3\text{PW}$ nanorod

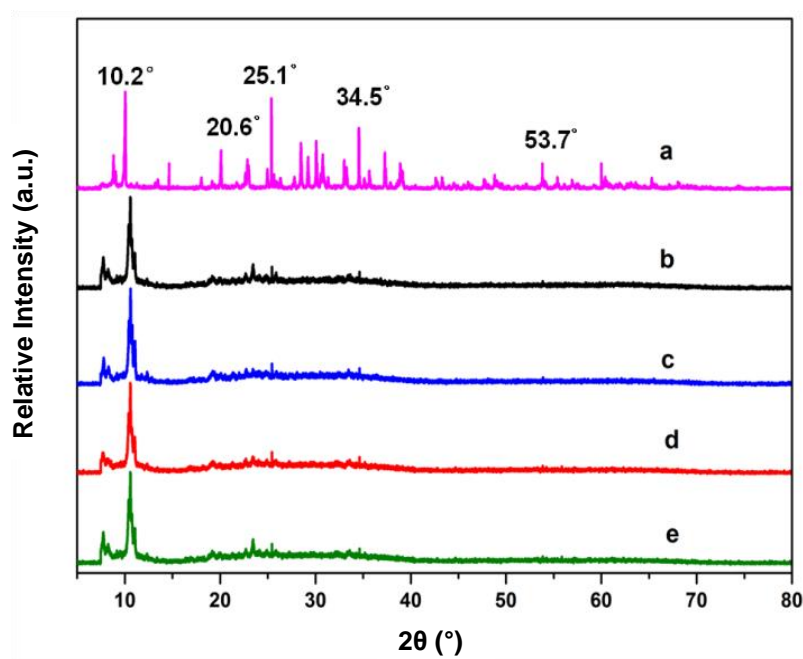


Fig. 3. XRD patterns of $(\text{CTA})_x\text{H}_{3-x}\text{PW}$ nanorod. (a) $\text{H}_3\text{PW}_{12}\text{O}_{40}$, (b) $(\text{CTA})\text{H}_2\text{PW}$ nanorod, (c) $(\text{CTA})_2\text{HPW}$ nanorod, (d) $(\text{CTA})_3\text{PW}$ nanorod, and (e) $(\text{CTA})\text{H}_2\text{PW}$ nanorod after the reaction

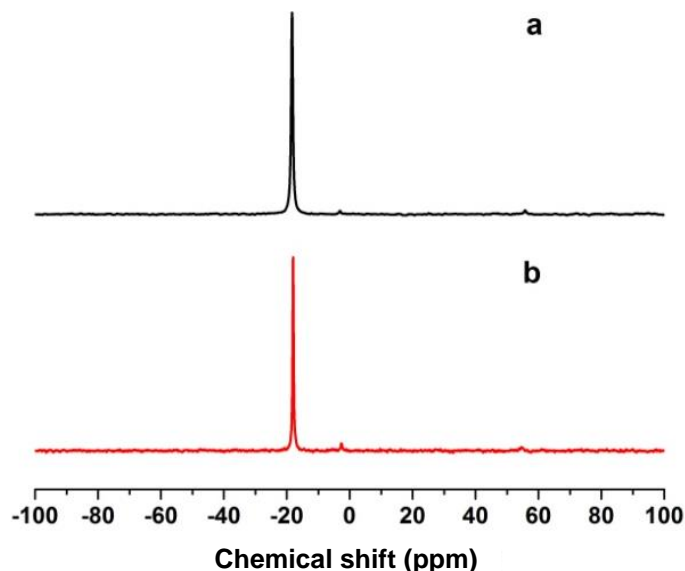


Fig. 4. ^{31}P MAS NMR spectrum of the (CTA) H_2PW nanorod (a) before the reaction, and (b) after the reaction

The SEM images of (CTA) H_2PW with different concentrations of CTAB and $\text{H}_3\text{PW}_{12}\text{O}_{40}$ determined the synthetic procedure of nanorods (Fig. 5). At lower concentrations, CTAB firstly reacted with $\text{H}_3\text{PW}_{12}\text{O}_{40}$ through ion exchanging reaction to form micellar sphere with size of 100 nm (Fig. 5a). Increasing their concentrations both to 15 mM, the micellar sphere grew bigger and then self-assembled at 20 mM to nanorods with diameters from 300 nm to 400 nm (Fig. 5b, 5c). When concentrations were further increased to 25 mM, the regular nanorod of (CTA) H_2PW was the main product in SEM with diameter of 500 nm (Fig. 5d). Furthermore, the ordered mesoporous structure of (CTA) H_2PW nanorod was determined by TEM (Fig. 6a). Combined with SEM and TEM, the self-assembly performance of CTAB and $\text{H}_3\text{PW}_{12}\text{O}_{40}$ was as follows: (1) CTA^+ reacted with $\text{H}_3\text{PW}_{12}\text{O}_{40}$ through ion-exchanging to (CTA) H_2PW single molecule; (2) (CTA) H_2PW self-assembled to form micellar sphere at lower concentrations; and (3) The obtained micelles were further stacked to form cylinders that were attached together as nanorod. The nanorod presented an ordered mesoporous structure (Scheme 1). From the IR and XRD of samples with different initial concentrations (Fig. 7), it could be concluded that such samples all showed the Keggin structure. This indicated that CTA^+ reacted with $\text{H}_3\text{PW}_{12}\text{O}_{40}$ firstly in a stoichiometric manner to (CTA) H_2PW , then it self-assembled into nanosphere or nanorod depending to the initial usages of CTAB and $\text{H}_3\text{PW}_{12}\text{O}_{40}$. The SEM images of (CTA) $_2\text{HPW}$ nanorod and (CTA) $_3\text{PW}$ nanorod are given in Fig. 8.

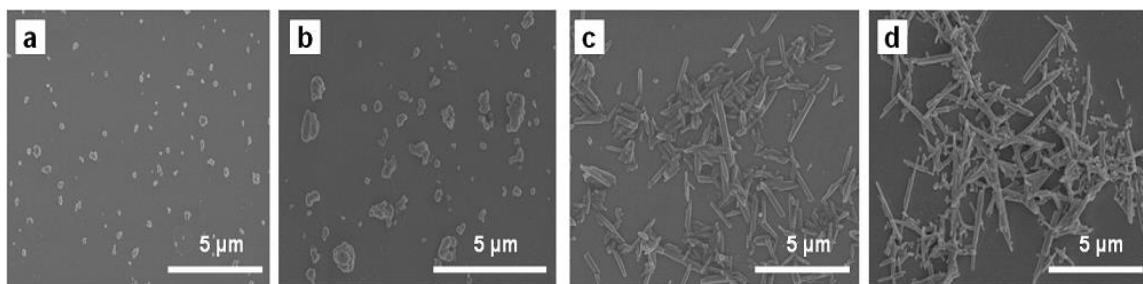
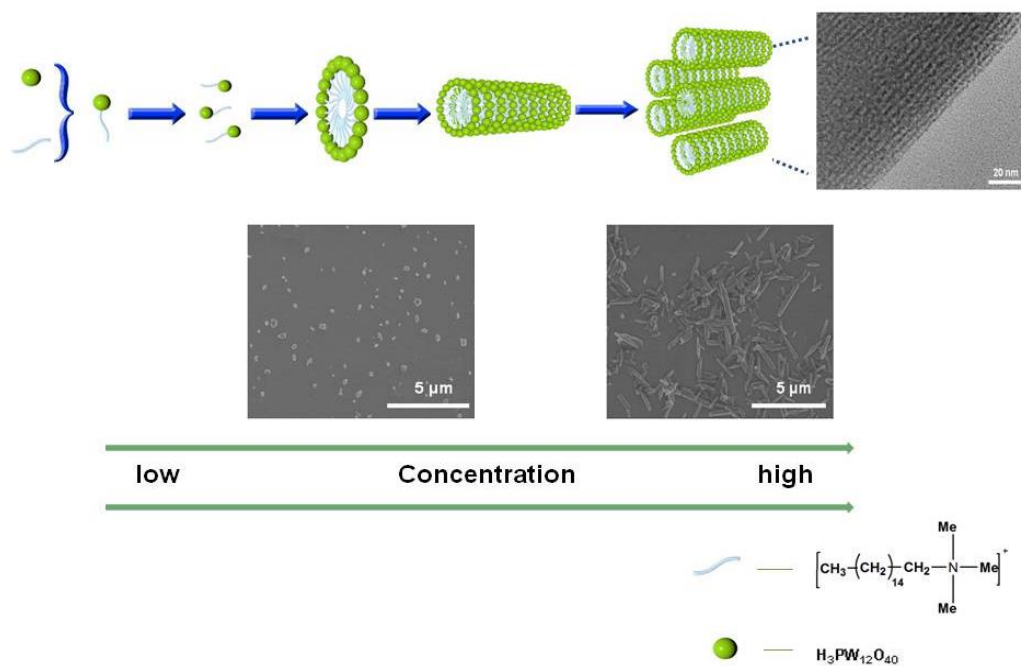


Fig. 5. SEM images of CTAB reacting with $H_3PW_{12}O_{40}$ with different concentrations of (a) 10 mM, (b) 15 mM, (c) 20 mM, and (d) 25 mM



Scheme 1. The synthetic procedures for $(\text{CTA})_x\text{H}_3\text{-}_x\text{PW}$ nanorod

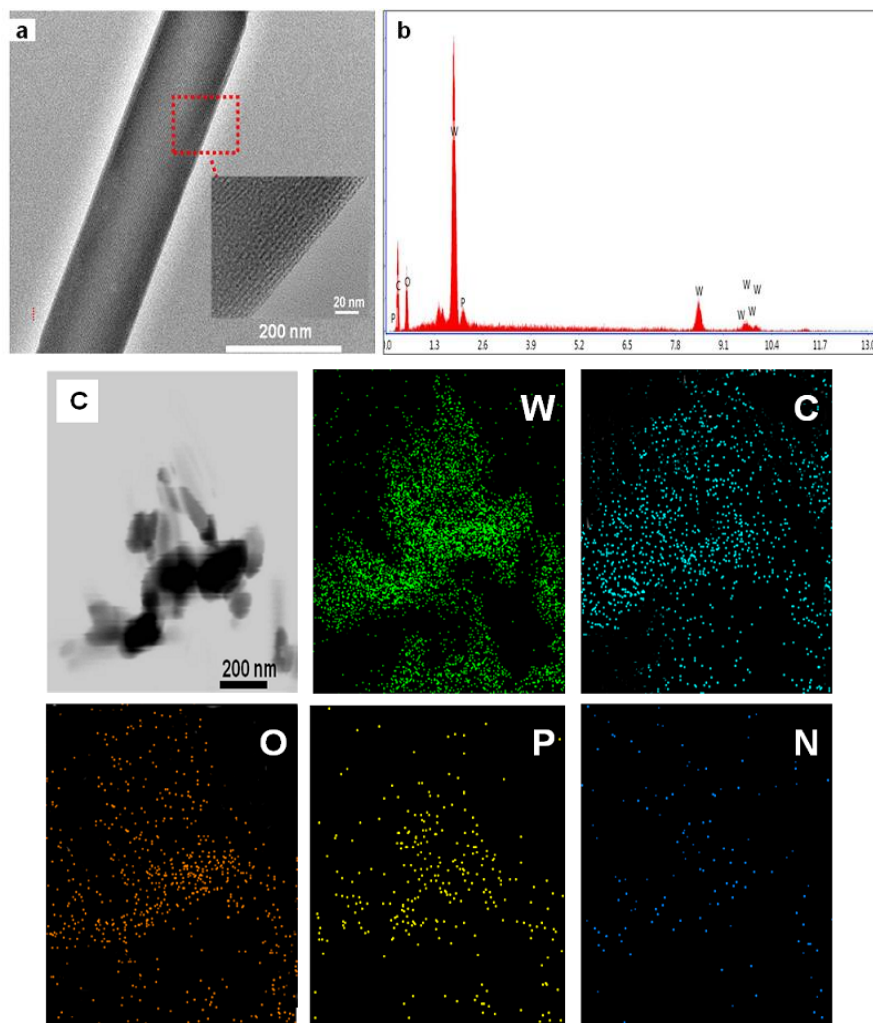


Fig. 6. The TEM image of (CTA) H_2PW nanorod at concentrations of 20 mM (a), EDX pattern (b), and compositional EDX mapping of the (CTA) H_2PW nanorod (c)

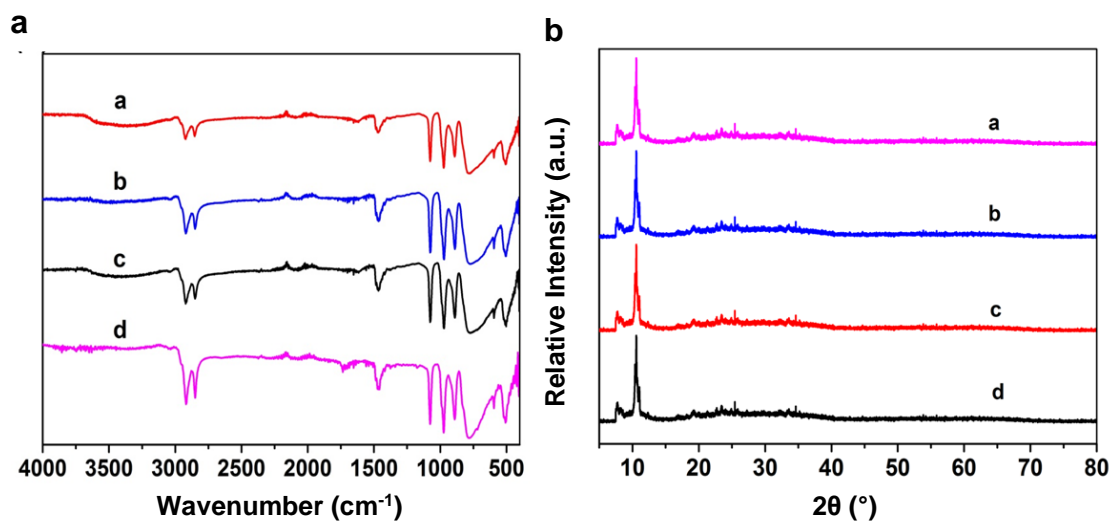


Fig. 7. IR spectra of and XRD patterns of CTAB reacting with $H_3PW_{12}O_{40}$ with different concentrations of (a) 10 mM, (b) 15 mM, (c) 20 mM, and (d) 25 mM

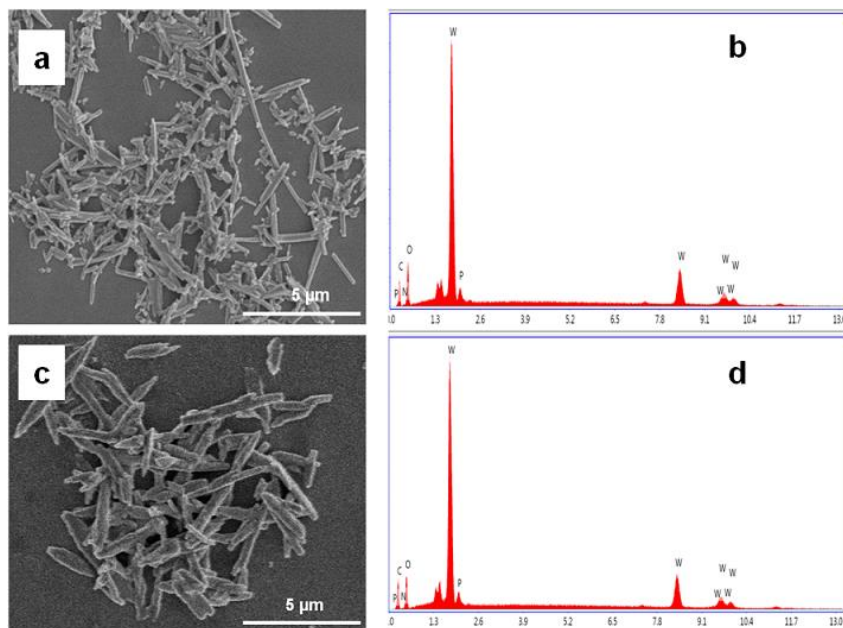


Fig. 8. The SEM image of $(\text{CTA})_2\text{HPW}$ nanorod (a) and EDX pattern (b), and the SEM image of $(\text{CTA})_3\text{PW}$ nanorod (c) and EDX pattern (d)

The energy dispersive X-ray spectroscopy (EDX) measurement (Fig. 6b) showed that the $(\text{CTA})\text{H}_2\text{PW}$ nanorod had no other impurities from the W, C, O, N, and P elements. The molar ratio of P and W obtained from the Fig. 6b was about 1:12, being consistent with the ICP elemental analysis, indicating that the $(\text{CTA})\text{H}_2\text{PW}$ nanorod maintained the Keggin structure. And the molar ratio of W to C was 12:19, indicating the formula of nanorod as $(\text{CTA})\text{H}_2\text{PW}$, which is coherent with elementary analysis. The energy dispersive spectroscopy (EDX) mapping (Fig. 6c) revealed a uniform dispersion of the component elements W, C, O, N, and P, demonstrating the strong interaction between CTA^+ and $\text{H}_3\text{PW}_{12}\text{O}_{40}$.

The N_2 adsorption-desorption isotherm and the pore size distribution of Barrett-Joyner-Halenda (BJH) for $(\text{CTA})\text{H}_2\text{PW}$ nanorod are given in Fig. 9. The sample exhibited a typical type IV isotherm and the relative pressure P/P_0 had a very pronounced H1 type hysteresis loop at 0.4 to 0.8, indicating that the prepared nanorod had a mesoporous structure. The pore size distribution of Barrett-Joyner-Halenda (BJH) indicated that the pore size of the catalyst was mainly distributed at 2.5 to 3 nm. The surface area of $(\text{CTA})\text{H}_2\text{PW}$ nanorod was $80.3 \text{ m}^2/\text{g}$.

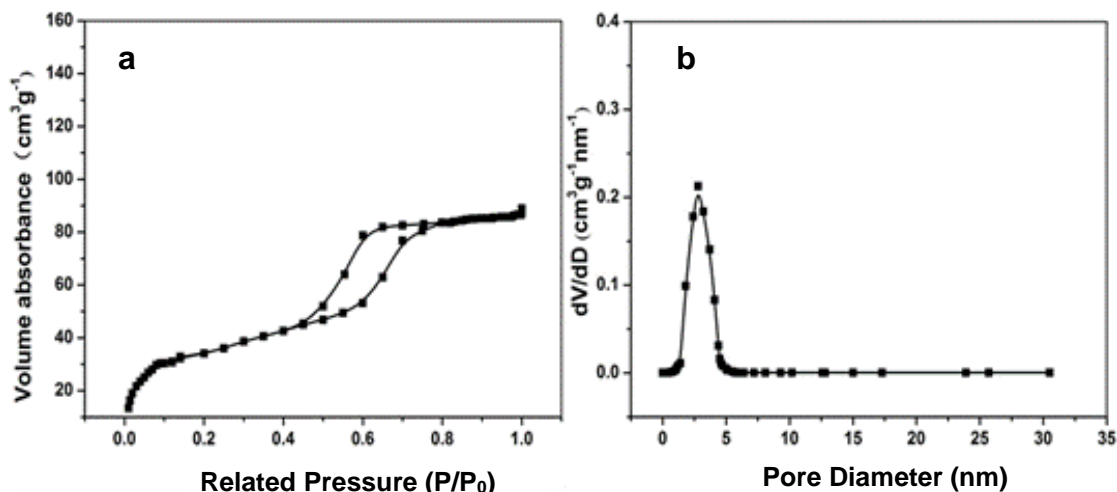


Fig. 9. (a) Nitrogen adsorption-desorption isotherm of (CTA)H₂PW nanorod, and (b) its BJH pore size distribution

Effect of Different Catalysts on Cellulose Hydrolysis

Firstly, the different catalysts were subjected to screening tests for cellulose hydrolysis in aqueous medium (Fig. 10). It could be clearly seen that without any catalyst, cellulose was hardly converted under the reaction conditions employed. In a previous report, micellar (CTA)H₂PW showed certain activity in cellulose hydrolysis, which presented 39.3% yield of glucose at 44.1% conversion in water at 170 °C for 8 h (Zhao 2011). It could be seen that the conversion of cellulose was improved to 64.8% in the presence of (CTA)H₂PW nanorods, while the yield of glucose also was increased to 54.3%. This improvement was attributed to its wire-like morphology (Zhang *et al.* 2016c) and higher surface area. The conversion of cellulose and yield of glucose also depended on the composition of the catalysts as (CTA)H₂PW > (CTA)₂HPW > (CTA)₃PW (Table 1), which was coherent with their acidic contents as (CTA)H₂PW (1.41 mmol/g) > (CTA)₂HPW (0.72 mmol/g) > (CTA)₃PW (0.04 mmol/g).

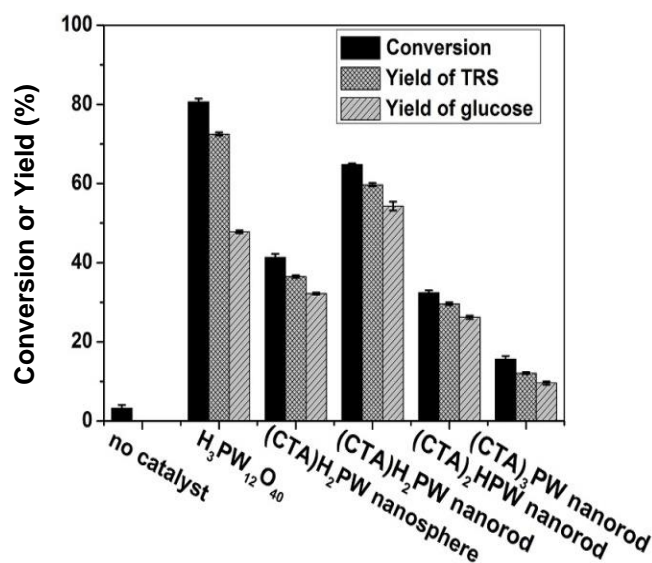
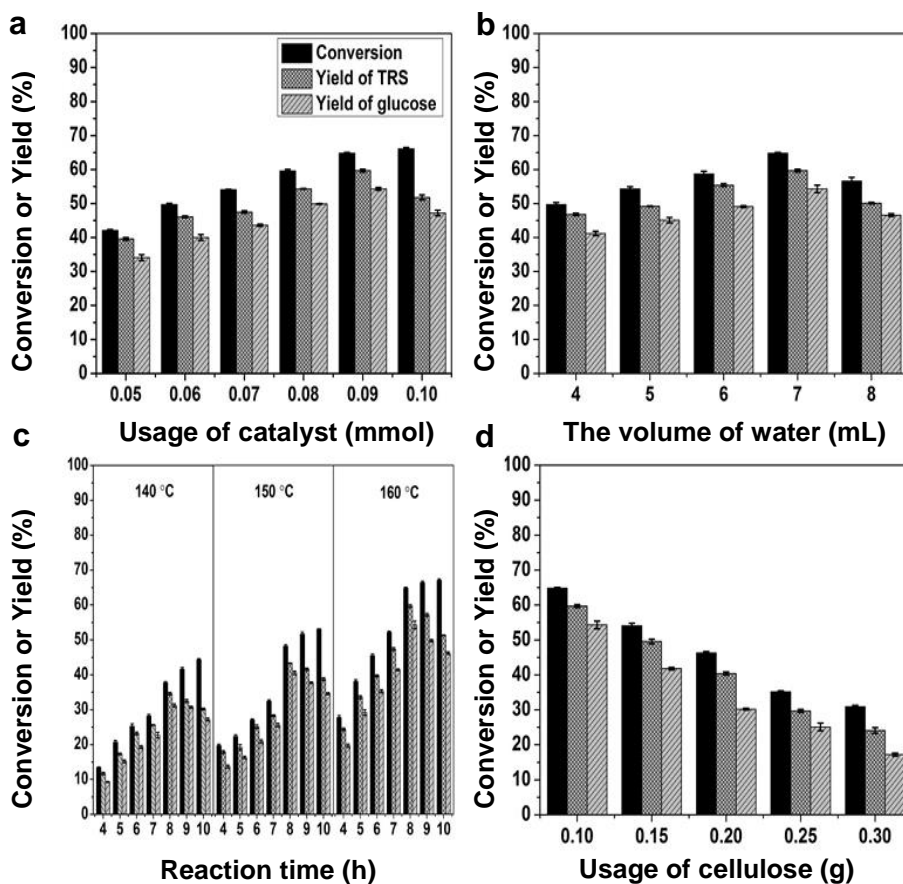


Fig. 10. Different catalysts on cellulose hydrolysis in water. Reaction conditions as 0.1 g of cellulose, catalyst (0.09 mmol), water (7 ml), 160 °C for 8 h

Due to its higher efficiency (CTA) H_2PW was used as the main catalyst in cellulose hydrolysis in water. The reaction conditions were optimized as usage of catalyst, volume of water, reaction temperature, reaction time, and different usage of cellulose (Fig. 11). It could be seen that the amount of catalyst increased from 0.05 mmol to 0.09 mmol (Fig. 11a). The conversion of cellulose and the yield of glucose were increased from 42.1% and 34.1% to 64.8% and 54.3%, respectively. This increase could be attributed to an increase in the active sites of the catalyst. However, when the amount of catalyst was increased to 0.1 mmol, the yield of glucose decreased to 47.2%, while conversion was not increased significantly. This decrease was attributable to the higher usage of catalyst, leading to further decomposition of glucose. Water was an essential reactant for the hydrolysis of cellulose. The yield of TRS and glucose increased with added volume of water from 4 mL to 7 mL (Fig. 11b). However, further increasing usage of water decreased the efficiency, which might be due to a reduction in acidic sites. Increasing the reaction time could increase the conversion rate, the yield of glucose increasing first and then decreasing, and the glucose yield reached the maximum at 8 h (Fig. 11c). As the temperature was increased from 140 to 160 °C, the conversion rate and glucose yield increased from 41.6% and 30.7% to 64.8% and 54.3%, respectively. The cellulose usages was increased from 0.1 g to 0.3 g with lowering yields, the usage of 0.1 g was chosen to be the optimum usage (Fig. 11d). In summary, the reaction conditions were optimized to be in 7 mL water at 160 °C for 8 h upon 0.09 mmol (CTA) H_2PW nanorod and 0.1 g of cellulose to give 54.3% yield of glucose at 64.8% cellulose conversion (Fig. 11).



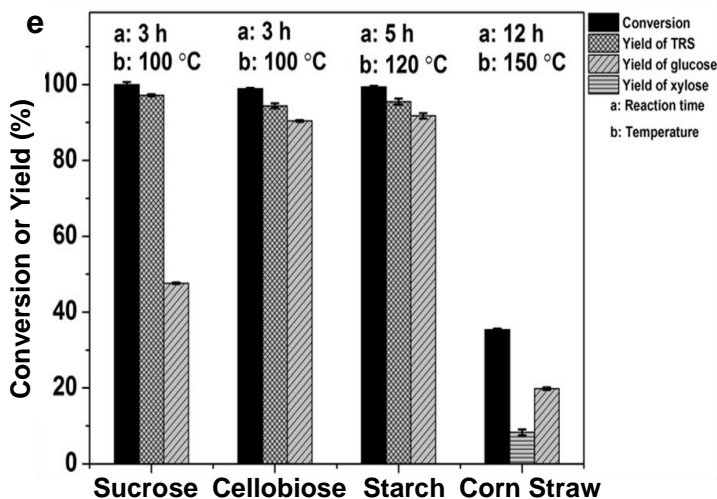


Fig. 11. The effect of (CTA)H₂PW nanorod under different reaction conditions: (a) usage of catalyst, (b) the volume of water, (c) temperature verse reaction time, (d) usage of cellulose, and hydrolysis for different feedstocks upon (CTA)H₂PW (e)

Other polysaccharides (sucrose, cellobiose, and starch), and lignocellulose (corn straw) were also achieved using (CTA)H₂PW nanorod as a catalyst under various reaction conditions (Fig. 11e). The yields of glucose were obtained as high as 47.6%, 89.4%, and 91.2%, corresponding to sucrose (containing 49.6% yield of fructose), cellobiose, and starch at ~100% conversion under various reaction conditions. (CTA)H₂PW nanorod showed potential for hydrolysis of polysaccharides to glucose. Beside polysaccharides, lignocellulose as corn straw had been used as feedstocks to produce value-added chemicals upon (CTA)H₂PW nanorod. The carbohydrates and lignin contents in corn straw samples were determined by the National Renewable Energy Laboratory (NREL) standard analytical procedure (Yang *et al.* 2019). The corn straw raw material contained cellulose 38.6%, hemicellulose 22.7%, and lignin 16.8%. Upon addition of (CTA)H₂PW nanorods, 19.8% yield of glucose and 8.3% yield of xylose at 35.4% conversion were obtained at 150 °C for 12 h. Up to this point, the best yield of glucose directly from Fenton-modified corn straw was achieved as 47.2% upon the ultralow enzyme combined with maleic acid and aluminum chloride under the reaction conditions as 45 °C for 48 h (Yang *et al.* 2019).

HMF is an important platform chemical, which has been produced directly from cellulose and lignocellulose in water or in water/MIBK biphasic system (Delidovich *et al.* 2016). So far, the best yields of HMF were 75.0% from cellulose and 27.6% from lignocellulose upon (HOCH₂CH₂N(CH₃)₃)H₂PW₁₂O₄₀ catalysts in water/MIBK system under the reaction conditions as 8 h at 140 °C (Zhang 2016c). And (CTA)H₂PW nanosphere showed some activity in hydrolysis of cellulose in water. In order to obtain 5-HMF, hydrolysis of cellulose was done in water/MIBK biphasic system in the presence of (CTA)H₂PW nanorod (Fig. 12). It could be seen without any catalyst, there was only 3.8% conversion for cellulose, and no glucose or 5-HMF were found. In the presence of H₃PW₁₂O₄₀, 91.2% conversion was obtained with yields for 5-HMF and glucose as 47.2 and 14.2%, indicating the essential of Brønsted acid sites in cellulose hydrolysis. The dependence of cellulose conversion and HMF yield on the Brønsted acidity further demonstrated this: (CTA)H₂PW nanorod (Con. ~100%, glucose yield 17.6%, and 5-HMF yield 57.2%) > (CTA)₂HPW nanorod (60.9%, 13.2%, and 29.1%) > (CTA)₃PW nanorod (32.7%, 7.9%,

and 14.3%). Compared to (CTA) H_2PW nanosphere, the conversion and HMF yield increased from 72.9% to ~100% and 36.3% to 57.2%, respectively. This showed that the morphology of nanorod might improve the conversion as well as 5-HMF yield. Another contribution was that the adsorption of cellulose and protection of 5-HMF were improved by (CTA) H_2PW nanorods (Fig. 13). (CTA) H_2PW nanorods presented higher activity than (CTA) H_2PW nanospheres did. The production of HMF from cellulose had been achieved in the $H_2O/MIBK$ system, including $AlCl_3 \cdot 6H_2O$ with 37.0% yield (Feng *et al.* 2018), HCl with 33.7% yield (Sweygers *et al.* 2018), $ChCl/H-Y$ with 55.0% yield (Peela *et al.* 2019), $NbPO-pH7$ with 16.2% yield (Zhang *et al.* 2015), PB_nNH_3Cl with 40.0% yield (Cao *et al.* 2015), betaine and $HCOOH$ with 26.0% yield (Delbecq *et al.* 2017), and $ZnCl_2$ with 80.6% yield (Zhang *et al.* 2016). On the other hand, the production of glucose from cellulose in water was achieved to give less than 32.1% yield upon some solid catalysts as TiO_2/SO_4^{2-} (Zhang *et al.* 2019), Nb/ZrO_2 (Gromov *et al.* 2017), and sulfonated carbon (Li *et al.* 2017). It could be concluded that (CTA) H_2PW nanorod played a significant role in cellulose hydrolysis, which was more active than most catalysts.

Favorable results also can be attributed to the fact that this catalyst had a linear shape and a pore structure, enriched a large amount of cellulose, and then increased contact with the active site, so that the reaction proceeded efficiently.

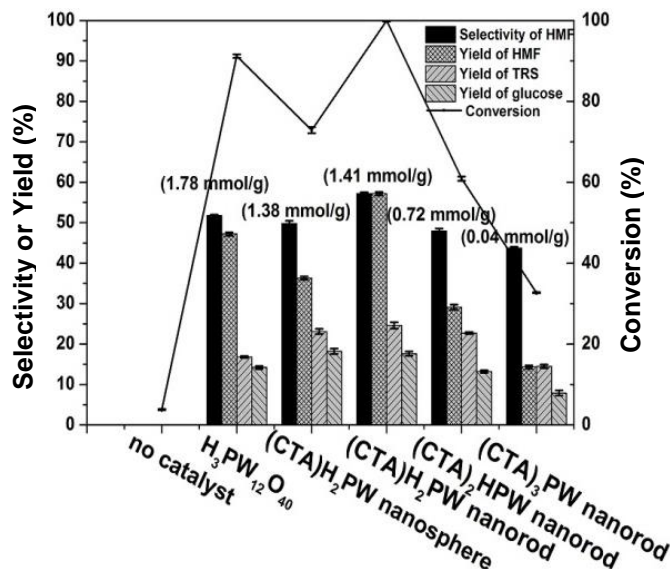


Fig. 12. Different catalysts on cellulose hydrolysis in biphasic system. Reaction conditions: 0.1 g of cellulose, catalysts (0.09 mmol), water (0.5 mL), MIBK (5 mL), 140 °C, 11 h

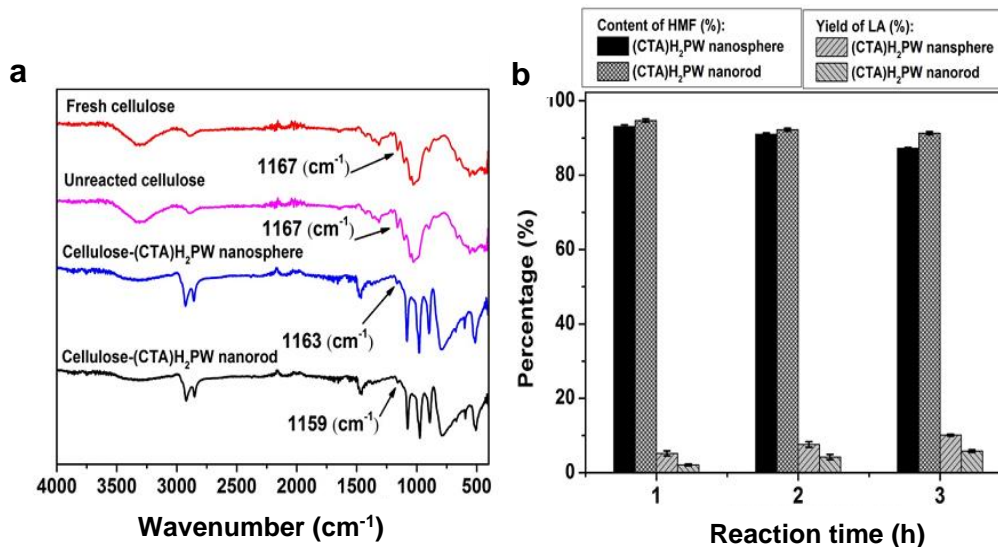


Fig. 13. (a) IR spectra of the fresh cellulose, the unreacted cellulose, the adsorption test of cellulose by (CTA)H₂PW nanosphere, and (CTA)H₂PW nanorod, and (b) the yield of LA and stability of 5-HMF combined with (CTA)H₂PW nanosphere and (CTA)H₂PW nanorod at 140 °C

The reaction conditions were optimized as temperature, reaction time, usage of the catalyst, concentration of cellulose (Fig. 14), and molar ratio of water to MIBK (Table 2). The hydrolysis of cellulose to HMF was studied at various temperatures and reaction times, as well as the yield of HMF and cellulose conversion over time at 130 to 150 °C (Fig. 14a-c). It could be seen that the reaction time and temperature had a great influence on the hydrolysis. Below 140 °C, the yield of HMF and the conversion of cellulose increased with the increase of time. Over 140 °C, the yield of HMF and the selectivity decreased, which was also ascribed to the side-reactions being predominant under higher temperature conditions. The conversion of cellulose and the yield of HMF reached a maximum of ~100% and 57.2% at 11 h.

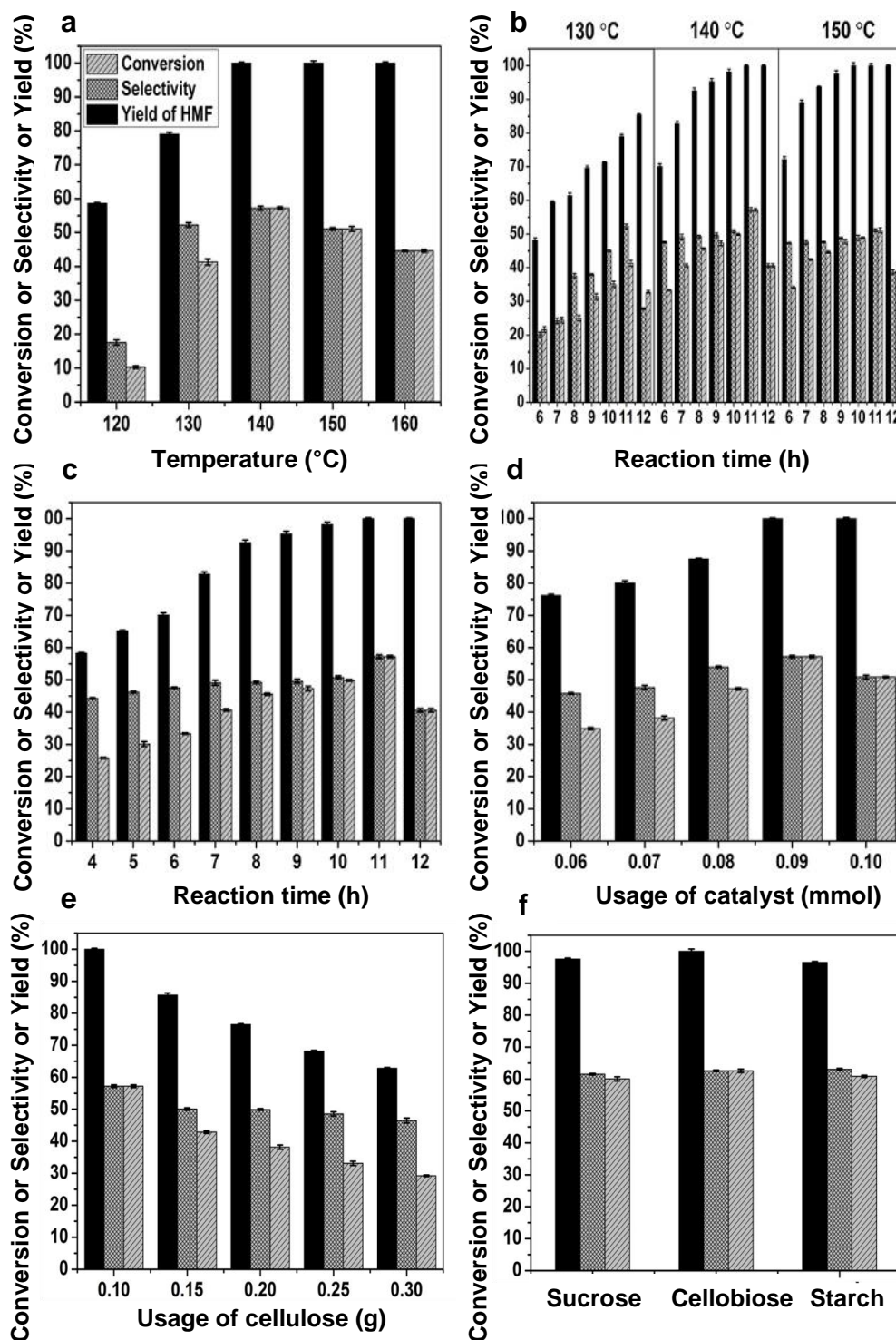


Fig. 14. The effect of (CTA)H₂PW nanorod under different reaction conditions: (a) reaction temperature, (b) temperature verse reaction time, (c) reaction time, (d) usage of catalyst, (e) usage of cellulose, and (f) the activity of (CTA)H₂PW nanorod on different substrates hydrolysis. Reaction conditions: sucrose (0.1 g), 120 °C, 5 h; cellobiose (0.1 g), 120 °C, 5 h; starch (0.1 g), 130 °C, 7 h

As the reaction time increased from 6 h to 11 h (Fig. 14b,c), such as at 140 °C, the conversion of cellulose and the yield of HMF increased from 70.1% and 33.3% to ~100%

and 57.2%, respectively, prolonging the reaction time to 12 h lowered yield due to the presence of by-products. The effect of catalyst usage on cellulose hydrolysis was explored by varying the amount of catalyst from 0.06 mmol to 0.09 mmol (Fig. 14d). Unexpectedly, the more the catalyst, the higher the conversion of cellulose. The conversion of cellulose and the yield of HMF increased from 76.2% and 34.9% to ~100% and 57.2%, with the changing of the amount of (CTA)H₂PW from 0.06 mmol to 0.09 mmol. Further increasing usage of catalyst to 0.1 mmol only led to decreasing trend of HMF yield, which was due to the dehydration of 5-HMF to levulinic acid. And the amount of cellulose had a certain effect on the hydrolysis of cellulose (Fig. 14e) at a range of 0.1 g to 0.3 g. The conversion of cellulose and the yield of HMF were able to reach a maxima of ~100% and 57.2% with 0.1 g cellulose. The volume ratio of H₂O to MIBK at 1: 10 was more suitable for 5-HMF generation (Table 2). As a result, the optimal conditions were as follows: 0.1 g cellulose and 0.09 mmol of catalyst in H₂O/MIBK = 1: 10 biphasic at 140 °C for 11 h with ~100% conversion of cellulose and 57.2% yield of 5-HMF.

Table 2. The Effect of Organic Solvent on the Hydrolysis of Cellulose to Form 5-HMF

Entry	Solvent (mL)	Con. (%)	Yield of 5-HMF (%)
1	H ₂ O (5.5)	54.8	4.2
2	MIBK (5.0)/H ₂ O (0.5)	~100	57.2
3	MIBK (4.7)/H ₂ O (0.8)	67.2	33.1
4	MIBK (4.5)/H ₂ O (1.0)	61.5	18.3
5	MIBK (4.0)/H ₂ O (1.5)	55.3	12.2
6	Acetone (5.0)/H ₂ O (0.5)	61.0	34.2
7	DMSO (5.0)/H ₂ O (0.5)	69.8	35.4
8	THF (5.0)/H ₂ O (0.5)	58.8	27.8
9	THF (5.5)	57.1	23.9
10	Acetone (5.5)	58.4	30.9
11	MIBK (5.5)	82.5	40.2
12	DMSO (5.5)	73.1	34.1

Beside cellulose, other polysaccharides including cellobiose, sucrose, and starch can be hydrolyzed in the presence of (CTA)H₂PW nanorod (Fig. 14f) in H₂O/MIBK biphasic. It could be seen that almost all polysaccharides could be converted under different conditions. (CTA)H₂PW nanorod showed 60.0% yield at 97.6% conversion for sucrose under 120 °C for 5 h, and 62.6% yield at ~100% conversion for cellobiose under 120 °C for 5 h, and 60.9% yield at 96.5% conversion for starch under 130 °C for 7 h.

Reusability of the Catalyst

Reusability was an important feature for heterogeneous catalysts while reducing costs. The way to assay life span of (CTA)H₂PW nanorod in cellulose system was explored in the following way: after the first run of the reaction finished, the residues of unreacted cellulose and the catalyst were separated by centrifuge and dried on air. In order to ensure the quality of the cellulose was 100 mg, a certain amount of fresh cellulose was refilled for the next reaction. The activity of the catalyst was still present after ten repeated experiments (Fig. 15). In water system, it showed the higher yields of glucose and the cellulose conversion in ten consecutive cycles (Fig. 15a). The catalyst

was recycled with a total leaching of only 9.5%. The cellulose conversion or the glucose yield was all reduced from 64.8% and 54.3% to 53.9% and 41.5%, respectively. In biphasic system, the conversion of cellulose and the yield of 5-HMF were 90.5% and 46.8% after ten cycles (Fig. 15b), respectively. After ten reaction runs, the total amount of (CTA)H₂PW nanorod leaching was only 9.1% of the initial usage. The stability of (CTA)H₂PW nanorod after the ten reactions was determined by IR spectroscopy (Fig. 1e).

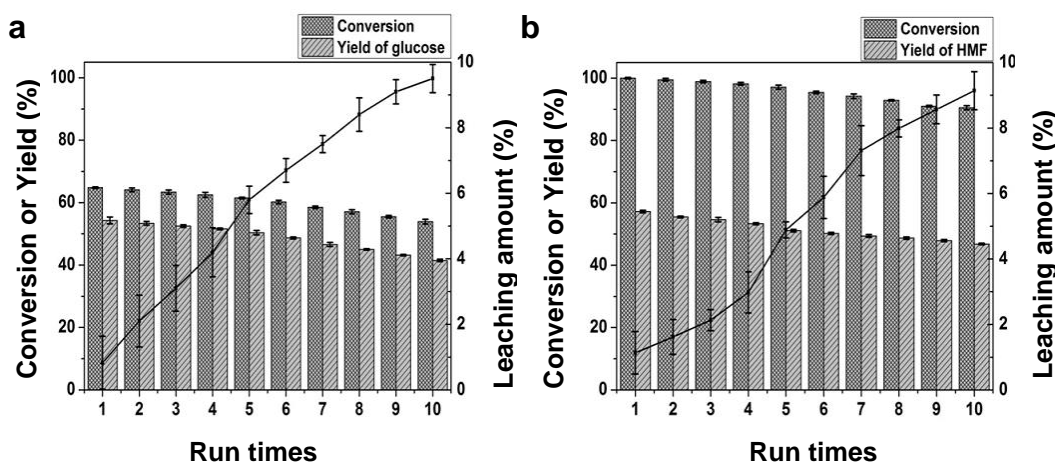


Fig. 15. The recycle tests of the catalyst under different reaction systems: (a) in water system, and (b) in biphasic system.

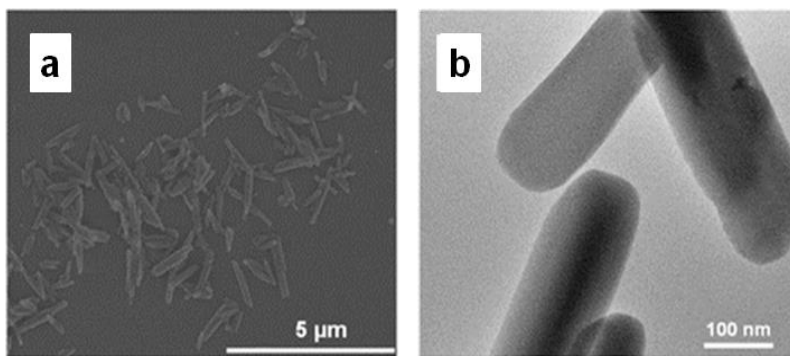


Fig. 16. (a) SEM image of the catalyst (CTA)H₂PW nanorod after the reaction, and (b) TEM image of (CTA)H₂PW nanorod after the reaction

There was no difference for the IR spectrum compared to that of a fresh one, which showed that the catalyst still kept the original Keggin structure during the reaction. And the IR spectra of the fresh cellulose and unreacted cellulose, since the solid catalyst and cellulose were inseparable, the IR spectrum of unreacted cellulose was measured by background removal, which showed the same main characteristic peaks at 3276, 2890, 1650, 1432, and 1167 cm^{-1} (Fig. 13a). Indicating that the structure of unreacted cellulose did not change during the reaction under such conditions. From the XRD powder diffraction pattern (Fig. 3e) and ³¹P MAS NMR spectrum (Fig. 4b) of the catalyst after the reaction, it could be seen that the structure and composition of the catalyst was not destroyed after the reaction, indicating the excellent stability of the (CTA)H₂PW nanorod

during the reaction. The SEM image and the TEM image (Fig. 16a, Fig. 16b) of the catalyst (CTA)₂PW nanorod after the reaction showed no significant change in the morphology. These results clearly indicated that (CTA)₂PW nanorod had excellent stability and produced 5-HMF activity without reducing after several ten repeated uses.

CONCLUSIONS

1. A series of novel mesoporous heteropolyacid nanorod catalysts (CTA)_xH_{3-x}PW (x = 1-3) was synthesized by surfactant encapsulation through simply controlling their initial concentration ratios of CTAB and H₃PW₁₂O₄₀. Particularly, the (CTA)₂PW nanorod showed a high specific surface area, mesoporous structure, one-dimensional morphology, and strong Brønsted acidity.
2. The catalytic effect was greatly improved compared to (CTA)₂PW with spherical morphology in conversion of cellulose to 5-HMF in the biphasic system with a yield of 57.2% and conversion of ~100% under the reaction conditions as 0.1 g cellulose and 0.09 mmol of catalyst in H₂O/MIBK = 1: 10 biphasic at 140 °C for 11 h. Meanwhile, 54.3% glucose could be obtained in hydrolysis of cellulose in water upon (CTA)₂PW nanorod. Such higher efficiency was contributed to its physical properties as linear structure with mesoporous, high specific surface area and Brønsted acidity.
3. The (CTA)₂PW nanorod showed easy separation, higher stability, and longer duration compared to (CTA)₂PW nanosphere, which could be reused for at least ten times without significant loss of activity.
4. (CTA)₂PW nanorod exhibited tolerance to feedstocks, which could catalyze lignocellulose of corn straw to glucose or xylose. This allowed (CTA)₂PW to be applied widely in conversion of cellulosic biomass into value-added chemical platform.

ACKNOWLEDGMENTS

This work was supported by the National Natural Science Foundation of China (No. 51578119), the major projects of Jilin Provincial Science and Technology Department (20180414069GH).

REFERENCES CITED

- Almohalla, M., Rodríguez Ramos, I., Ribeiro, L. S., Órfão, J. J. M., Pereira, M. F. R., and Guerrero Ruiz, A. (2018). "Cooperative action of heteropolyacids and carbon supported Ru catalysts for the conversion of cellulose," *Catal. Today* 301, 65-71. DOI: 10.1016/j.cattod.2017.05.023
- Bao, Y. Y., Bi, L. H., Wu, L. X., Mal, S. S., and Kortz, U. (2009). "Preparation and characterization of Langmuir-Blodgett films of wheel-shaped Cu-20 tungstophosphate and DODA by two different strategies," *Langmuir*. 25(22), 13000-

13006. DOI: 10.1021/la901854e
- Bu, W. F., Uchida, S., and Mizuno, N. (2009). "Micelles and vesicles formed by polyoxometalate-block copolymer composites," *Angew. Chem.* 121(44), 8431-8434. DOI: 10.1002/anie.200904116
- Cao, X. Q., Teong, S. P., Wu, D., Yi, G. S., Su, H. B., and Zhang, Y. G. (2015). "An enzyme mimic ammonium polymer as a single catalyst for glucose dehydration to 5-hydroxymethylfurfural," *Green Chem.* 17(4), 2348-2352. DOI: 10.1039/c4gc02488e
- Carraro, M., Sartorel, A., Scorrano, G., Maccato, C., Dickman, M. H., Kortz, U., and Bonchio, M. (2008). "Chiral Strandberg-type molybdates $[(RPO_3)_2Mo_5O_{15}]^{2-}$ as molecular gelators: Self-assembled fibrillar nanostructures with enhanced optical activity," *Angew. Chem. Int. Ed.* 47, 7275-7279. DOI: 10.1002/anie.200801629
- Chambon, F., Rataboul, F., Pinel, C., Cabiac, A., Guillon, E., and Essayem, N. (2011). "Cellulose hydrothermal conversion promoted by heterogeneous Brønsted and Lewis acids: Remarkable efficiency of solid Lewis acids to produce lactic acid," *Appl. Catal. B: Environ.* 105(1-2), 171-181. DOI: 10.1016/j.apcatb.2011.04.009
- Cheng, M. X., Shi, T., Guan, H. Y., Wang, S. T., Wang, X. H., and Jiang, Z. J. (2011). "Clean production of glucose from polysaccharides using a micellar heteropolyacid as a heterogeneous catalyst," *Appl. Catal. B: Environ.* 107(1-2), 104-109. DOI: 10.1016/j.apcatb.2011.07.002
- Cowan, J. J., Bailey, A. J., Heintz, R. A., Do, B. T., Hardcastle, K. I., Hill, C. L., and Weinstock, I. A. (2001). "Formation, isomerization, and derivatization of Keggin tungstoaluminates," *Inorg. Chem.* 40(26), 6666-6675. DOI: 10.1021/ic0106120
- Delbecq, F., Wang, Y. T., and Len, C. (2017). "Various carbohydrate precursors dehydration to 5-HMF in an acidic biphasic system under microwave heating using betaine as a co-catalyst," *Molecular Catal.* 434, 80-85. DOI: 10.1016/j.mcat.2017.02.037
- Delidovich, I., Leonhard, K., and Palkovits, R. (2014). "Cellulose and hemicellulose valorisation: An integrated challenge of catalysis and reaction engineering," *Energy Environ.* 7(9), 2803-2830. DOI: 10.1039/C4EE01067A
- Delidovich, I., Hausoul, P.J.C., Deng, L., Pfützner, R., Rose, M., and Palkovits, R. (2016). "Alternative monomers based on lignocellulose and their use for polymer production," *Chem. Rev.* 116(3), 1540-1599. DOI: 10.1021/acs.chemrev.5b00354
- Deng, W. P., Zhang, Q. H., and Wang, Y. (2012). "Polyoxometalates as efficient catalysts for transformations of cellulose into platform chemicals," *Dalton T.* 41(33), 9817-9831. DOI: 10.1039/c2dt30637a
- Deltcheff, C. R., Fournier, M., Franck, R., and Thouvenot, R. (1983). "Vibrational investigations of polyoxometalates. 3. Isomerism in molybdenum(VI) and tungsten(VI) compounds related to the Keggin structure," *Inorg. Chem.* 22, 207-216. DOI: 10.1021/ic00173a022
- Duan, X., Sun, G., Sun, Z., Li, J., Wang, S., Wang, X., Li, S., and Jiang, Z. (2013). "A heteropolyacid-based ionic liquid as a thermoregulated and environmentally friendly catalyst in esterification reaction under microwave assistance," *Catal. Commun.* 42, 125-128. DOI: 10.1016/j.catcom.2013.08.014
- Fan, C. Y., Guan, H. Y., Zhang, H., Wang, J. H., Wang, S. T., and Wang, X. H. (2011). "Conversion of fructose and glucose into 5-hydroxymethylfurfural catalyzed by a solid heteropolyacid salt," *Biomass Bioenerg.* 35, 2659-2665. DOI: 10.1016/j.biombioe.2011.03.004

- Feng, Y. C., Li, M. Z., Gao, Z. B., Zhang, X., Zeng, X. H., Sun, Y., Tang, X., Lei, T. Z. and Lin, L. (2018). "Development of betaine-based sustainable catalyst for green conversion of carbohydrates and biomass into 5-hydroxymethylfurfural," *ChemSusChem*. 12, 495-502. DOI: 10.1002/cssc.201802342
- Geboers, J., Stijn, V. D. V., Carpentier, K., De Blochouse, K., and Jacobs, P. (2010). "Efficient catalytic conversion of concentrated cellulose feeds to hexitols with heteropoly acids and Ru on carbon," *Sels B. Chem. Commun.* 46(20), 3577-3579. DOI: 10.1039/c001096k
- Gromov, N. V., Taran, O. P., Semeykina, V. S., Danilova¹, I. G., Pestunov, A. V., Parkhomchuk, E. V., and Parmon, V. N., (2017). "Solid acidic NbO_x/ZrO₂ catalysts for transformation of cellulose to glucose and 5-hydroxymethylfurfural in pure hot water," *Catal. Lett.* 147,1485-1495. DOI 10.1007/s10562-017-2056-y
- Jing, S. S., Cao, X. F., Zhong, L. X., Peng, X. W., Sun, R. C., and Liu, J. C. (2018). "Effectively enhancing conversion of cellulose to HMF by combining in-situ carbonic acid from CO₂ and metal oxides," *Ind. Crop. Prod.* 126, 151-157. DOI: 10.1016/j.indcrop.2018.10.028
- Kang, Z. H., Wang, E. B., Jiang, M., and Lian, S. Y. (2004). "Synthesis and characterization of polyoxometalate nanowires based on a novel microemulsion process," *Nanotechnology* 15(1), 55-58. DOI: 10.1088/0957-4484/15/1/010
- Kumar, V. B., Pulidindi, I. N., Mishra, R. K., and Gedanken, A. (2016). "Development of Ga salt of molybdophosphoric acid for biomass conversion to levulinic acid," *Energy Fuel* 30(12), 10583-10591. DOI: 10.1021/acs.energyfuels.6b02403
- Li, X. C., Peng, K. H., Xia, Q., Liu, X. H., and Wang, Y. Q. (2018). "Efficient conversion of cellulose into 5-hydroxymethylfurfural over niobia/carbon composites," *Chem. Eng.* 332, 528-536. DOI: 10.1016/j.cej.2017.06.10
- Li, C., Jiang, Z. X., Gao, J. B., Yang, Y. X., Wang, S. H., Tian, F. P., Sun, F. X., Sun, X. P., Ying, P. L., and Han, C. R. (2004). "Ultra-deep desulfurization of diesel: Oxidation with a recoverable catalyst assembled in emulsion," *Chem. Eur. J.* 10(9), 2277-2280. DOI: 10.1002/chem.200305679
- Li, H. L., Sun, H., Qi, W., Xu, M., and Wu, L. X. (2007). "Onionlike hybrid assemblies Based on surfactant-encapsulated polyoxometalates," *Angew. Chem.* 119(8), 1322-1325. DOI: 10.1002/anie.200603934
- Li, O. L., Ikura, R. and Ishizaki, T. (2017). "Hydrolysis of cellulose to glucose over carbon catalysts sulfonated via a plasma process in dilute acids," *Green Chem.* 19, 4774-4777. DOI: 10.1039/c7gc02143g
- Liu, S. Q., Kurth, D. G., Bredenkötter, B., and Volkmer, D. (2002). "The structure of self-assembled multilayers with polyoxometalate nanoclusters," *Am. J. Chem. Soc.* 124(41), 12279-12287. DOI: 10.1021/ja026946l
- Lü, H. Y., Zhang, Y. N., Jiang, Z. X., and Li, C. (2010). "Aerobic oxidative desulfurization of benzothiophene, dibenzothiophene and 4,6-dimethyldibenzothiophene using an Anderson-type catalyst [(C₁₈H₃₇)₂N(CH₃)₂]₅[IMo₆O₂₄]," *Green Chem.* 12, 1954-1958. DOI: 10.1039/C0GC00271B
- Nisar, A., Zhuang, J., and Wang, X. (2009a). "Cluster-based self-assembly: Reversible formation of polyoxometalate nanocones and nanotubes," *Chem. Mater.* 21(16), 3745-3751. DOI: 10.1021/cm901305r
- Nisar, A., Xu, X. X., Shen, S. L., Hu, S., and Wang, X. (2009b). "Noble metal nanocrystal-incorporated fullerene-like polyoxometalate based microspheres," *Adv.*

- Funct. Mater.* 19(6), 860-865. DOI: 10.1002/adfm.200801580
- Nisar, A., Lu, Y., and Wang, X. (2009c). "Assembling polyoxometalate clusters into advanced nanoarchitectures," *Chem. Mater.* 22(11), 3511-3518. DOI: 10.1021/cm100691a
- Nisar, A., Lu, Y., Zhuang, J., and Wang, X. (2011). "Polyoxometalate nanocone nanoreactors: Magnetic manipulation and enhanced catalytic performance," *Angew. Chem.* 123(14), 3245-3250. DOI: 10.1002/anie.201006155
- Palkovits, R., Tajvidi, K., Ruppert, A. M., and Procelewska, J. (2011). "Heteropoly acids as efficient acid catalysts in the one-step conversion of cellulose to sugar alcohols," *Chem. Commun.* 47(1), 576-578. DOI: 10.1039/c0cc02263b
- Peela, N. R., Yedla, S. K., Velag, B., Kumar, A., and Golder, A. K. (2019). "Choline chloride functionalized zeolites for the conversion of biomass derivatives to 5-hydroxymethylfurfural," *Appl. Catal. A: Gen.* 580, 59-70. DOI: 10.1016/j.apcata.2019.05.005
- Pizzio, L. R., and Blanco, M. N. (2007). "A contribution to the physicochemical characterization of nonstoichiometric salts of tungstosilicic acid," *Micropor. Mesopor. Mater.* 103, 40-47. DOI: 10.1016/j.micromeso.2007.01.036
- Qu, Y. S., Huang, C. P., Zhang, J., and Chen, B. H. (2012). "Efficient dehydration of fructose to 5-hydroxymethylfurfural catalyzed by a recyclable sulfonated organic heteropolyacid salt," *Bioresour. Technol.* 106, 170-172. DOI: 10.1016/j.biortech.2011.11.069
- Ritchie, C., Cooper, G. J. T., Song, Y. F., Streb, C., Yin, H. B., Parenty, A. D. C., MacLaren, D. A., and Cronin, L. (2009). "Spontaneous assembly and real-time growth of micron-scale tubular structures from polyoxometalate-based Inorganic solids," *Nat. Chem.* 1, 47-52. DOI: 10.1038/nchem.113
- Sun, Z., Cheng, M. X., Li, H. C., Shi, T., Yuan, M. J., Wang, X. H., and Jiang, Z. J. (2012). "One-pot depolymerization of cellulose into glucose and levulinic acid by heteropolyacid ionic liquid catalysis," *RSC Adv.* 2(24), 9058-9065. DOI: 10.1039/C2RA01328B
- Sun, Z., Tao, M. L., Zhao, Q., Guang, H. Y., Shi, T., and Wang, X. H. (2015a). "A highly active willow-derived sulfonated carbon material with macroporous structure for production of glucose," *Cellulose* 22(1), 675-682. DOI: 10.1007/s10570-014-0540-8
- Sun, Z., Zhang, X. Y., Wang, S. T., Li, X. Y., Wang, X. H., and Shi, J. Y. (2015b). "Hydrolysis and alcoholysis of polysaccharides with high efficiency catalyzed by $(C_{16}TA)_xH_{6-x}P_2W_{18}O_{62}$ nanoassembly," *RSC Adv.* 5, 94155-94163. DOI: 10.1039/C5RA15047G
- Sun, Z., Xue, L. F., Wang, S. T., Wang, X. H., and Shi, J. Y. (2016). "Single step conversion of cellulose to levulinic acid using temperature-responsive dodecaaluminotungstic acid catalysts," *Green Chem.* 18(3), 742-752. DOI: 10.1039/C5GC01730K
- Sweygers, N., Harrer, J., Dewil, R., and Appels, L. (2018). "A microwave-assisted process for the in-situ production of 5-hydroxymethylfurfural and furfural from lignocellulosic polysaccharides in a biphasic reaction system," *J. Clean. Prod.* 187, 1014-1024. DOI: 10.1016/j.jclepro.2018.03.204
- Tang, N. F., Zhang, Y. N., Lin, F., Lü, H. Y., Jiang, Z. X., and Li, C. (2012). "Oxidation of dibenzothiophene catalyzed by $[C_8H_{17}N(CH_3)_3]_3H_3V_{10}O_{28}$ using molecular oxygen as oxidant," *Chem. Commun.* 48, 11647-11649. DOI: 10.1039/c2cc36482d
- Tsubaki, S., Oono, K., Ueda, T., Onda, A., Yanagisawa, K., Mitani, T., and Azuma, J. I.

- (2013). "Microwave-assisted hydrolysis of polysaccharides over polyoxometalate clusters," *Bioresource Technol.* 144, 67-73. DOI: 10.1016/j.biortech.2013.06.092
- Wang, H. F., Fang, L. P., Yang, Y. F., Zhang, L., and Wang, Y. J. (2016). "H₅PMo₁₀V₂O₄₀ immobilized on functionalized chloromethylated polystyrene by electrostatic interactions: A highly efficient and recyclable heterogeneous catalyst for hydroxylation of benzene," *Catal. Sci. Technol.* 6, 8005-8015. DOI: 10.1039/C6CY01270A
- Xie, X., Han, J. Y., Wang, H., Zhu, H., Liu, X., Niu, Y. F., Song, Z. Q., and Ge, Q. F. (2014). "Selective conversion of microcrystalline cellulose into hexitols over a Ru/[Bmim]₃PW₁₂O₄₀ catalyst under mild conditions," *Catal. Today* 233, 70-76. DOI: 10.1016/j.cattod.2013.09.061
- Yang, M., Jin, C. D., Shuang, E., Liu, J. L., Zhang, S., Liu, Q. Y., Sheng, K. C., and Zhang, X. M. (2019). "Fenton reaction-modified corn stover to produce value-added chemicals by ultralow enzyme hydrolysis and maleic acid and aluminum chloride catalytic conversion," *Energy Fuel* 33(7), 6429-6435. DOI: 10.1021/acs.energyfuels.9b00983
- Zhao, S., Cheng, M. X., Li, J. Z., Tian, J., and Wang, X. H. (2011). "One pot production of 5-hydroxymethylfurfural with high yield from cellulose by a Brønsted-Lewis-surfactant-combined heteropolyacid catalyst," *Chem. Commun.* 47, 2176-2178. DOI: 10.1039/c0cc04444j
- Zhao, S. Q., Xu, G. Z., Chang, C., Fang, S. Q., Liu, Z., and Du, F. G. (2013). "Direct conversion of carbohydrates into ethyl levulinate with potassium phosphotungstate as an efficient catalyst," *Catal.* 5(4), 1897-1910. DOI: 10.3390/catal5041897
- Zhao, Q., Sun, Z., Wang, S. T., Huang, G. H., Wang, X. H., and Jiang, Z. J. (2014). "Conversion of highly concentrated fructose into 5-hydroxymethylfurfural by acid-base bifunctional HPA nanocatalysts induced by choline chloride," *RSC Adv.* 4(108), 63055-63061. DOI: 10.1039/C4RA10121A
- Zhao, P. P., Zhang, Y. Y., Wang, Y., Cui, H. Y., Song, F., Sun, X. Y., and Zhang, L. P. (2018a). "Conversion of glucose into 5-hydroxymethylfurfural catalyzed by acid-base bifunctional heteropolyacid-based ionic hybrids," *Green Chem.* 20(7), 1551-1559. DOI: 10.1039/C7GC03821F
- Zhao, J. J., Zhang, Y. L., Wang, K., Yan, C. H., Da, Z. L., Li, C. X., and Yan, Y. S. (2018b). "Development of hierarchical porous MOF-based catalyst of UiO-66(Hf) and its application for 5-hydroxymethylfurfural production from cellulose," *ChemistrySelect* 3(41), 11476-11485. DOI: 10.1002/slct.201802423
- Zhang, J., Song, Y. F., Cronin, L., Liu, T. B., and Am, J. (2008). "Self-assembly of organic-inorganic hybrid amphiphilic surfactants with large polyoxometalates as polar head groups," *J. Am. Chem. Soc.* 130(44), 14408-14409. DOI: 10.1021/ja805644a
- Zhang, Y., Wang, J. J., Li, X. C., Liu, X. H., Xia, Y. J., Hu, B. C., Lu, G. Z., and Wang, Y. Q. (2015). "Direct conversion of biomass-derived carbohydrates to 5-hydroxymethylfurfural over water-tolerant niobium-based catalysts," *Fuel* 139, 301-307. DOI: 10.1016/j.fuel.2014.08.047
- Zhang, Y. N., Lü, H. Y., Wang, L., Zhang, Y. L., Liu, P., Han, H. X., Jiang, Z. X., and Li, C. (2010). "The oxidation of benzothiophene using the Keggin-type lacunary polytungstophosphate as catalysts in emulsion," *J. Mol. Catal. A: Chem.* 332, 59-64. DOI: 10.1016/j.molcata.2010.08.021
- Zhang, Y. M., Degirmenci, V., Li, C., and Hensen, E. J. M. (2011). "Phosphotungstic

- acid encapsulated in metal-organic framework as catalysts for carbohydrate dehydration to 5-hydroxymethylfurfural," *ChemSusChem*. 4(1), 59-64. DOI: 10.1002/cssc.201000284
- Zhang, X. Y., Zhang, D., Sun, Z., Xue, L. F., Wang, X. H., and Jiang, Z. J. (2016a). "Highly efficient preparation of HMF from cellulose using temperature-responsive heteropolyacid catalysts in cascade reaction," *Appl. Catal. B: Environ.* 196, 50-56. DOI: 10.1016/j.apcatb.2016.05.019
- Zhang, Y. L., Pan, J. M., and Shen, Y. T. (2016b). "HIPes template: Towards the synthesis of polymeric catalysts with adjustable porous structure, acid-base strength and wettability for biomass energy conversion," *Chem. Eng. J.* 283, 956-970. DOI: 10.1016/j.cej.2015.08.090
- Zhang, Y. R., Li, N., Li, M. F., and Fan, Y. M. (2016c). "Highly efficient conversion of microcrystalline cellulose to 5-hydroxymethyl furfural in a homogeneous reaction system," *RSC Adv.* 6, 21347-21351. DOI: 10.1039/c5ra22129c
- Zhang, Z. F., Sadakane, M., Hiyoshi, N., Yoshida, A., Hara, M., and Ueda, W. (2016c). "Acidic ultrafine tungsten oxide molecular wires for cellulosic biomass conversion," *Angew. Chem. Int. Ed.* 55(35), 10234-10238. DOI: 10.1002/ange.201602770
- Zhang, Y. L., Jin, P., Liu, M., Pan, J. M., and Yan, Y. S. (2017). "A novel route for green conversion of cellulose to HMF by cascading enzymatic and chemical reactions," *AIChE J.* 63(11), 4920-4932. DOI: 10.1002/aic.15841
- Zhang, X. Y., Zhang, H. Z., Li, Y. M., Bawa, M., Wang, S. T., Wang, X. H., and Jiang, Z. J. (2018). "First triple-functional polyoxometalate Cs_{10.6}[H_{2.4}GeNb₁₃O₄₁] for highly selective production of methyl levulinate directly from cellulose," *Cellulose* 25, 6405-6419. DOI: 10.1007/s10570-018-2037-3
- Zhang, X. Y. L., Lu, H. F., Wu, K. J., Liu, Y. Y., Liu, C. J., Zhu, Y. M., and Liang, B. (2019). "Hydrolysis of mechanically pre-treated cellulose catalyzed by solid acid SO₄²⁻-TiO₂ in water-ethanol solvent," *Chin. J. Chem. Eng.* DOI: 10.1016/j.cjche.2019.02.027
- Zhang, X. Y., Zhang, X. Y., Sun, N. Y., Wang, S. T., Wang, X. H., and Jiang, Z. J. (2019). "High production of levulinic acid from cellulosic feedstocks being catalyzed by temperature-responsive transition metal substituted heteropolyacids," *Renew. Energ.* 141, 802-813. DOI: 10.1016/j.renene.2019.04.058
- Zheng, H. W., Sun, Z., Yi, X. H., Wang, S. T., Li, J. X., Wang, X. H., and Jiang, Z. J. (2013). "A water-tolerant C₁₆H₃PW₁₁CrO₃₉ catalyst for the efficient conversion of monosaccharides into 5-hydroxymethylfurfural in a micellar system," *RSC Adv.* 3(45), 23051-23056. DOI: 10.1039/c3ra43408g

Article submitted: July 31, 2019; Peer review completed: October 19, 2019; Revised version received: November 4, 2019; Accepted: November 5, 2019; Published: November 13, 2019.

DOI: 10.15376/biores.15.1.240-264